EPJ Web of Conferences **35**, 06001 (2012)
DOI: 10.1051/epjconf/20123506001

Towards the pair spectroscopy of the Hoyle state in ^{12}C

T. Kibédi[1,a], A.E. Stuchbery[1], G.D. Dracoulis[1], and K.A. Robertson[1]
[1] Department of Nuclear Physics, The Australian National University, ACT 0200, Australia

Abstract. The triple–alpha process leading to the formation of stable carbon in the Universe is one of the most important nuclear astrophysical processes. The radiative width of the so–called Hoyle state, involving the 7.654 MeV E0 and the 3.2148 MeV E2 transitions, is known with 10–12% accuracy. A novel, more direct approach to determining the width is proposed here, based on the measurement of the E0 and the E2 internal pair conversion intensities. We report on the development of a new magnetic pair spectrometer with high sensitivity for electron–positron pairs and with excellent energy resolution.

1 Introduction

Carbon, the fourth most abundant element in the Universe, is produced through the triple–alpha process. In the stellar environment, two α particles (^{4}He nuclei) fuse to form the highly unstable nucleus ^{8}Be, which has a halflife of only 6.7×10^{-17} s for decay back to two α particles. Occasionally, a third α particle combines with the ^{8}Be before the decay takes place, forming a cluster of three α particles. At the right energy, these α–particles form a 7.654 MeV resonant state, the Hoyle state, in the stable nucleus ^{12}C (see Fig. 1). However 99.96% of the time the resonant state decays back to ^{8}Be by alpha emission, producing no stable carbon nuclei. The remaining 0.04% of the time it decays to one of two lower energy states in ^{12}C. This rare decay is the only path for the formation of carbon in the universe. Since the original prediction of the existence of a second 0^+ state in ^{12}C by Fred Hoyle [1] in 1953, this state has been of great interest, not only in nuclear synthesis, but also in nuclear structure and reactions. Its existence was experimentally confirmed soon afterward [2]. However, the structure of the Hoyle state is still not understood in detail.

The decay pathways of the Hoyle state are illustrated in Fig. 1. Because γ–ray emission is forbidden for transitions between two 0^+ states, this pathway (E0) can only take place via internal conversion and/or pair production. Calculations show that for a 7.654 MeV E0 transition, the dominant process will be pair conversion. For the 3.2148 MeV E2 decay to the intermediate 2^+ state, γ radiation occurs 99.9% of the time, with pair conversion mainly responsible for the remaining decays.

[a] e-mail: Tibor.Kibedi@anu.edu.au

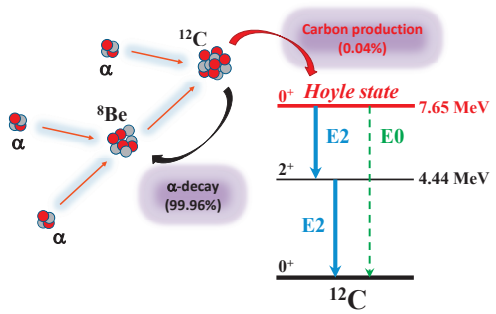

Fig. 1. 3α–process and the formation of ^{12}C.

The total rate of ^{12}C producing decays from the Hoyle state depends directly on the *radiative width* $\Gamma_{\rm rad}$, which includes the width for γ emission (Γ_γ), for internal conversion ($\Gamma_{\rm CE}$), and for pair production (Γ_π); *i.e.*

$$\Gamma_{\rm rad} = \Gamma_\gamma^{\rm E2} + \Gamma_\pi^{\rm E0} + \Gamma_\pi^{\rm E2} + \Gamma_{\rm CE}^{\rm E0} + \Gamma_{\rm CE}^{\rm E2}\,. \qquad (1)$$

The rate $r_{3\alpha}$ for the triple–alpha reaction [3] can be written as

$$r_{3\alpha} \propto \Gamma_{\rm rad}\ \exp(-Q_{3\alpha}/kT), \qquad (2)$$

where $Q_{3\alpha}$ is the energy released in the α decay of the Hoyle state and T is the temperature. In previous studies $\Gamma_{\rm rad}$ has been determined as a product of three independently measured quantities:

$$\Gamma_{\rm rad} = \left[\frac{\Gamma_{\rm rad}}{\Gamma}\right] \times \left[\frac{\Gamma}{\Gamma_\pi^{\rm E0}}\right] \times \left[\Gamma_\pi^{\rm E0}\right]. \qquad (3)$$

The total width of the Hoyle state, Γ is defined as the sum of the radiative and the alpha decay widths: $\Gamma = \Gamma_\alpha + \Gamma_{\rm rad}$. The currently adopted $\Gamma_{\rm rad}/\Gamma$, Γ_π^{E0}/Γ and Γ_π^{E0} values are summarized in Table 1. The largest contribution to the uncertainty in the triple α rate is from $\Gamma_\pi^{\rm E0}/\Gamma$ (8.9%) followed by Γ_π^{E0} (8.8%). The later one is dominated by a large, $6\times\sigma$ difference between the two most recent measurements of $\Gamma_\pi^{\rm E0}$ by Crannell *et al.* [4] and Chernykh *et al.* [5]. Further studies are required to resolve the discrepancy between these two measurements, which use electron scattering methods.

The new approach is based on measuring the relative intensities of the E0 and E2 transitions and using $\Gamma_\pi^{\rm E0}$, the only absolutely known quantity in Eqn. 3. The observation of the pair conversion is the only feasible decay channel which can be used. We estimate that Γ_π^{E0} carries about 1.5% of Γ_{rad} and Γ_π^{E2} is in the order of 0.09%. Through the measurements of $\Gamma_\pi^{\rm E2}/\Gamma_\pi^{\rm E0}$ we plan to determine $\Gamma_{\rm rad}$ from:

$$\Gamma_{rad} = \left[\frac{\Gamma_\pi^{\rm E2}}{\Gamma_\pi^{\rm E0}}\right] \times \left[\left(1 + \frac{1}{\alpha_\pi^{\rm E2}}\right) + 1\right] \times \left[\Gamma_\pi^{\rm E0}\right], \qquad (4)$$

Table 1. Adopted experimental values required to determine Γ_{rad} from Eqn. 3.

$\Gamma_{rad}/\Gamma \times 10^4$	**4.13(11)**
Alburger (1961) [7]	3.3(9)
Seeger & Kavanagh (1963) [8]	2.8(3)[(a)]
Hall & Tanner (1964) [9]	3.5(12)
Chamberlin *et al.* (1974) [10]	4.2(2)
Davids *et al.* (1975) [11]	4.30(20)
Mark *et al.* (1975) [12]	4.15(34)
Markham *et al.* (1976) [13]	3.87(25)
Obst *et al.* (1976) [14]	4.09(29)
$\Gamma_\pi/\Gamma \times 10^6$	**6.75(60)**
Alburger (1961) [7]	6.9(21)
Obst *et al.* (1972) [15]	6.9(23)
Alburger (1977) [16]	7.1(8)
Robertson *et al.* (1977) [17]	6.0(11)
$\Gamma_\pi^{E0} \times 10^{-5}\, eV$	**5.7(5)**
Fregau (1956) [18]	5.5(30)
Crannell & Griffy (1964) [19]	6.5(7)
Gudden & Strehl (1965) [20]	7.3(13)
Crannell *et al.* (1967) [21]	6.2(6)
Strehl & Schucan (1968) [22]	6.4(4)[(b)]
Strehl (1970) [23]	5.94(51)
Crannell *et al.* (2005) [4]	5.20(14)
Chernykh *et al.* (2010) [5]	6.23(20)

[(a)] Outlier, data excluded.
[(b)] Superceeded, data excluded.

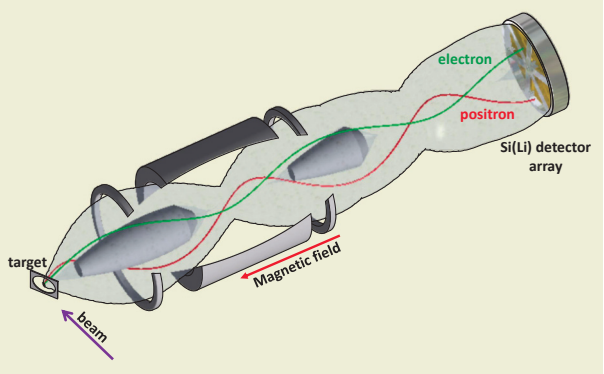

Fig. 2. (Color online) Schematic view of the magnetic pair spectrometer. (Courtesy of Caleb Gudu, ANU)

where $\alpha_\pi^{E2} = 8.766 \times 10^{-4}$ is the theoretical pair conversion coefficient, known with an accuracy of ≈ 1 % [6]. The last term in Eqn. 4, Γ_π^{E0}, will be taken from the literature. The currently available data is summarised in Table 1.

Test experiments have been carried out with the absorber system used for conversion electron spectroscopy [24] combined with an array of six Si(Li) detectors of 4.2 mm thickness used for e–e coincidence measurements [25]. Some of the results of this initial measurement have been reported elsewhere [26]. Here we report on the development of the new magnetic pair spectrometer.

2 Design of the new pair spectrometer

The Hoyle state will be populated in the laboratory using the $^{12}C(p, p')^{12}C(7.654\ \text{MeV})$ reaction at 10.5 MeV, a resonant bombarding energy [27]. Electron–positron pairs

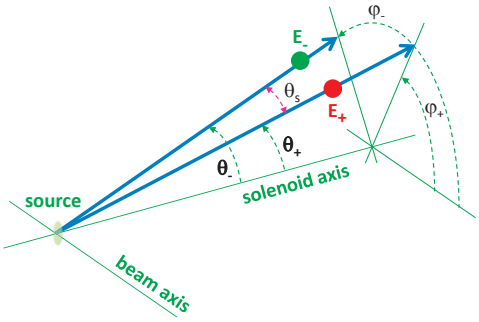

Fig. 3. (Color online) Geometry used in the trajectory calculations.

will be recorded using the ANU Super-e electron spectrometer [24] augmented with an array of Si(Li) detectors as shown in Fig. 2. The 2.1 Tesla superconductive solenoid is mounted perpendicular to beam of the 14UD Heavy Ion accelerator. The target is rotated at 45 degrees to the beam direction allowing the beam to pass through and the transportation of electrons and/or positrons (referred here as *"particles"*) from the rear of the target. For a given magnetic field the two axial baffles and the diaphragm (Fig. 2) define an energy range of particles which can reach the detector. A key element of the new pair spectrometer is a Si(Li) array, consisting of six pie–shaped detectors, located at 35 cm distance from the target, where most of the particles will complete two and a half loops. In this arrangement, a valid pair event is defined as one in which any pair of the six detectors has fired and the summed energy of the two particles, E_+ and E_- satisfies the relation:

$$\omega = E_+ + E_- + 2 \times m_\circ c^2\,, \tag{5}$$

where ω is the transition energy and $m_\circ c^2$ is the electron rest mass. Due to the selectivity of the magnetic transporter, both particles, the electron and positron, can only reach the detector if they have similar kinetic energies. The pair spectrometer will sample a well defined energy window centered around $(\omega - 2 \times m_\circ c^2)/2$.

Electrons and positrons share the available kinetic energy and are ejected with a separation angle, θ_s. The double differential of the emission probability, $d^2P_\pi/dE_+d\theta_s$ depends on the atomic number, transition energy, multipolarity as well as E_+ and θ_s. The relevant emission rates for the 7.654 MeV E0 and 3.2148 MeV E2 transitions have been evaluated [28] using the Born approximation, which is a sufficiently accurate approach for a relatively low Z value and for cases when $E_+ \approx E_-$. For electric monopole transitions the pair conversion probability, $P_\pi(Z, \omega)$, is

$$P_\pi(Z, \omega) = \rho^2(0_i^+ \rightarrow 0_f^+) \times \Omega_\pi(Z, \omega)\,. \tag{6}$$

The monopole transition strength ρ^2 is a dimensionless parameter for an E0 transition between the initial (0_i^+) and final (0_f^+) states and depends only on the nuclear structure [29]. On the other hand, the so–called electronic factor, $\Omega_\pi(Z, \omega)$ [30] does not depend on nuclear properties. Its second derivative, $d^2\Omega_\pi/dE_+d\theta_s$ can be calculated using the formulae given by Oppenheimer [31]:

$$\frac{d^2\Omega_\pi(Z,\omega)}{dE\ d\cos\theta_s} = p_+p_-(W_+W_- - m_\circ^2c^4 + p_+p_-c^2\cos\theta_s)\,, \tag{7}$$

where p_+ (p_-) and W_+ (W_-) are the positron (electron) momenta and total energy. To take into account the effect of the nuclear Coulomb field a small correction [32] was also applied. The distribution of the theoretical $d^2\Omega_\pi/dE_+d\theta_s$ values over the full positron energy and separation angle parameter space is shown for the 7.654 MeV E0 transition in the upper panel of Fig. 4. It peaks for equal energy sharing and for a separation angle of $\sim 60°$.

For multipole transitions with $L > 0$, the differential pair conversion coefficient, $d^2\alpha_\pi/dE_+ d\cos\theta$ is defined as:

$$\frac{d^2\alpha_\pi(Z,\omega,\tau L)}{dE\ d\cos\theta_s} = \frac{d^2P_\pi(Z,\omega,\tau L)/dE\ d\cos\theta_s}{P_\gamma(Z,\omega,\tau L)}, \quad (8)$$

where $d^2P_\pi(Z,\omega,\tau L)/dE\ d\cos\theta_s$ is the double differential probability of the pair emission. $P_\gamma(Z,\omega,\tau L)$ is the photon emission probability. The lower frame of Fig. 4 shows the probability distribution for the 3.2148 MeV E2 transition, as was evaluated using the Born approximation [33] with a Coulomb correction [6]. For the E2 transition the distribution is a much sharper function of the separation angle than the one is for the E0 transition. It peaks at $\theta_s \sim 30°$. On the other hand, it is less sensitive to the positron energy (E_+), but approximately equal energy sharing is still favoured. There is a slight tendency for $E_+ > E_-$ due to the Coulomb field.

In the absence of detailed tabulations of the double differential $\Omega_\pi(E0)$ and $\alpha_\pi(E2)$ values, Eqns 7 and 8 will be used to evaluate the pair conversion efficiency of the spectrometer. By comparing the $d\alpha_\pi(E2)/dE_+$ (single differential) values with those from ref. [34,35], we found that for $Z = 6$ and for cases when $E_- \approx E_+$ the above approximations are accurate to better than 1%.

Central to the development of the new pair spectrometer (Fig. 2) was the evaluation of the transportation of the electron–positron pairs. A modified version of the original Monte Carlo code, developed for conversion electron measurements [24], was used. A new emission module was added, which samples the probability distributions (Eqns. 6 and 8) using randomly selected E_+ and θ_s values. The initial take–off angles defined in Fig. 3 (θ_-, θ_+, ϕ_-, ϕ_+) are randomly selected and the trajectories for both particles are evaluated in the axially symmetric magnetic field using the Runge–Kutta method. Typical particle trajectories (coloured lines) as well as the envelope of all trajectories for a fixed magnetic field ("cloud") are shown in Fig. 2. The initial experiments demonstrated [26], that the pair spectrometer works and that the main source of the background is the high energy photons from the target itself. This is dominated by the 4.439 MeV E2 transition from the first excited state in ^{12}C. Using extensive simulations, a new absorber system has subsequently been designed. The shape of the two axial absorbers and diaphragm has been set to maximise the electron–positron pair efficiency and the material between the target and the Si(Li) detectors. The absorbers are made from Heavymet (a non–magnetic tungsten alloy) with a minimum thickness of 8.2 cm to shield high energy photons. To minimise the scattering of electrons and positrons, as well as to reduce the production of photoelectrons, a thin (1–2 mm) layer of low Z material (epoxy resin, Torr Seal) was added to the absorbers and to the diaphragm.

Representative results of the simulations for the 7.654 MeV E0 and for the 3.2148 MeV E2 transitions are shown

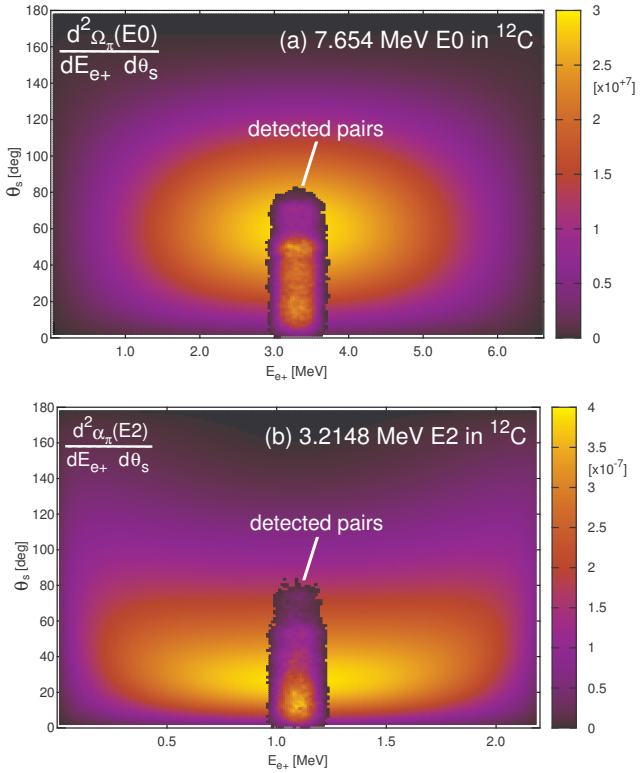

Fig. 4. (Color online) Calculated double differential pair emission rates for *(a)* the 7.654 MeV E0 and *(b)* the 3.2148 MeV E2 transitions in ^{12}C. The distribution of simulated events of electron–positron pairs detected with the magnetic pair spectrometer is also shown (*"detected pairs"*).

Table 2. Selected spectrometer parameters for the pair spectroscopy of the Hoyle state. 1 Million electron–positron pair events (for each case) were used to determine optimum parameters for the 3.2148 MeV E2 and 7.654 MeV E0 in ^{12}C.

Warm bore diameter	84.3 mm
Source to detector distance	350 mm
Detector active area [(a)]	236 mm^2
Detector thickness	9 mm
Acceptance (take off) angles θ_-, θ_+	15.9° – 46.9°
Absolute efficiency[(a)]	0.50 %/4π
3.2148 MeV E2	
Optimum magnetic field	0.19607 Tesla
Combined efficiency[(b)]	
Pairs hitting different detector segments	0.0720 %/4π
Pairs hitting same detector segment	0.0076 %/4π
7.654 MeV E0	
Optimum magnetic field	0.47047 Tesla
Combined efficiency[(b)]	
Pairs hitting different detector segments	0.0694 %/4π
Pairs hitting same detector segment	0.0013 %/4π

(a) For one of the six detector segments.
(b) For all 15 combinations of detector pairs.

in Fig. 4 and Table 2. These are based on 500,000 simulated events in each case. The distribution of electron–positron pairs, when both particles hit different detector segments, are superimposed on the theoretical distribution of pair emission in Fig. 4 and labelled as *"detected pairs"*. For clarity, these distributions were constructed from the initial coordinates of the pairs. The figure illustrates the well defined window centered at the energy of $[\omega - (2 \times m_\circ c^2)]/2$. The distributions are much wider along the separation angle, θ_s, reaching a maximum value just lower than the optimum separation angle of $\sim 60^\circ$ for E0 and $\sim 30^\circ$ for E2. There is also a finite probability that both particles will hit the same segment, which will be registered as a single event at the energy of $\omega - 2 \times m_\circ c^2$.

3 Conclusion

A new magnetic pair spectrometer is being developed for the spectroscopy of the electromagnetic transitions from the Hoyle state in ^{12}C. It combines a homogenous magnetic lens with a new array of six Si(Li) detectors mounted in a well shielded location. The design of the spectrometer is expected to be completed in 2012 and a series of experiments using radioactive sources and well known reactions are planned to test the new spectrometer.

Acknowledgement

This work was supported by the Australian National University Major Equipment Grant scheme, Grant No 11MEC15 (2011).

References

1. F. Hoyle, *et al.*, *Phys. Rev.* **92** (1953) 1095 N6
2. D.N.F. Dunbar, *et al.*, Phys. Rev. **92** (1953) 649
3. C.E. Rolfs and W.S. Rodney, *Cauldrons in the cosmos: nuclear astrophysics*, Chicago, University of Chicago Press, (1988)
4. H. Crannell, *et al.*, *Nucl. Phys.* **A 758** (2005) 399c
5. M. Chernykh, *et al.*, Phys. Rev. Lett. **105** (2010) 022501
6. P. Schlüter, G. Soff, W. Greiner, Phys. Rep. **75** (1981) 327
7. D.E. Alburger, Phys. Rev. **124** (1961) 193
8. P.A. Seeger, R.W. Kawanash, Astrophys. J. **137** (1963) 704
9. I. Hall and N.W. Tanner, Nucl. Phys. **53** (1964) 673
10. D. Chamberlin, *et al.*, Phys. Rev. **C9** (1974) 69
11. C.N. Davids, *et al.*, Phys. Rev. **C11** (1975) 2063
12. H.B. Mak, *et al.*, Phys. Rev. **C12** (1975) 1158
13. R.G. Markham, *et al.*, Nucl. Phys. **A270** (1976) 489
14. A.W. Obst and W.J. Braithwaite, Phys. Rev. **C13** (1976) 2033
15. A.W. Obst, *et al.*, Phys. Rev. **C5** (1972) 738
16. D.E. Alburger, Phys. Rev. **C16** (1977) 2394
17. R.G.H. Robertson, *et al.*, Phys. Rev. **C15** (1977) 1072
18. J.H. Fregeau, Phys. Rev. **104** (1956) 225
19. H.L. Crannell and T.A. Griffy, Phys. Rev. **136** (1964) B1580
20. F. Gudden and P. Strehl, Z. Phys. **185** (1965) 111
21. H. Crannell, *et al.*, Nucl. Phys. **A90** (1967) 152
22. P. Strehl and T.H. Schucan, Phys. Lett. **B27** (1968) 641
23. P. Strehl, Z. Phys. **234** (1970) 416
24. T. Kibédi, G.D. Dracoulis and A.P. Byrne, *Nucl. Instr. and Meth. in Phys. Res.* **A294** (1990) 523
25. K.H. Maier, *et al.*, Phys. Rev. **C76** (2007) 6
26. T. Kibédi, *et al.* Proc. of the Fourteenth Internat. Symp. on Capture Gamma–Ray Spectroscopy and Related Topics, Guelph, August 28 - September 2, 2011, (World Scientific in press)
27. C.N. Davids and T.I. Bonner, Asrophis. J. **166** (1971) 405
28. K.A. Robertson, ASC reseseach project, Australian National University (2008)
29. T. Kibédi and R.H. Spear, At. Data Nucl. Data Tables **89** (2005) 77
30. E.L. Church and J. Weneser, Phys. Rev. **103** (1956) 1035
31. J.R. Oppenheimer, Phys. Rev. **60** (1941) 159
32. D.H. Wilkinson, Nucl. Phys. **A133** (1969) 1
33. M.E. Rose, Phys. Rev. **76** (1949) 678
34. P. Schluter and G. Soff, At. Data Nucl. Data Tables **24** (1979) 509
35. Ch. Hofmann, *et al.*, Phys. Rev. **C42** (1990) 2632